International Journal of Mass Spectrometry 277 (2008) 52–56

Contents lists available at ScienceDirect

International Journal of Mass Spectrometry

journal homepage: www.elsevier.com/locate/ijms

Dissociation and fragmentation of furan by electron impact

Marcin Dampc, Mariusz Zubek*

Department of Physics of Electronic Phenomena, Gdańsk University of Technology, Narutowicza 11/12, 80-952 Gdańsk, Poland

ARTICLE INFO

Article history:
Received 17 March 2008
Received in revised form 11 April 2008
Accepted 16 April 2008
Available online 24 April 2008

Keywords:
Fragmentation process
Electron impact
Dissociative excitation
Fluorescence emission

ABSTRACT

Dissociation and fragmentation processes that produce electronically excited atomic and molecular fragments, following electron impact excitation, have been studied in furan. The optical excitation technique has been employed over the electron incident energy range 15–95 eV. Formation of excited hydrogen atoms H(n) in the n = 4–10 states has been detected by observation of the Balmer series. The diatomic CH fragments are formed in the $A^2\Delta$, $B^2\Sigma^-$ and $C^2\Sigma^-$ electronic states and the C_2 fragments in the $d^3\Pi_g$ excited state. The appearance energies for the H(n = 4) (H_β line) and the CH($A^2\Delta$) ($A^2\Delta \rightarrow X^2\Pi_r$ transition) fragments have been measured to be 20.7 ± 0.4 and 19.0 ± 0.3 eV, respectively. Absolute emission cross sections have been also determined for the above two transitions in the electron energy range from the appearance energy thresholds up to 95 eV. Possible dissociation and fragmentation processes are discussed.

1. Introduction

The furan molecule belongs to a series of the five-membered heterocyclic compounds which are relevant in biochemistry and also in industry [1]. Its heterocyclic structure incorporates an oxygen atom (Fig. 1) and has a high degree of aromaticity. The molecule in the ground state (X^1A_1) is classified in the C_{2v} symmetry point group. The furan ring can be considered as a building unit in the biologically active compounds, vitamin B12, biotin [2] and polymers [3]. It could be also seen as a simplified ring model analogue of the deoxyribose molecule in the DNA backbone structure and studies of its interactions with low energy electrons are crucial for the understanding of radiation damage in biological tissue [4].

There is a very limited amount of work performed on the dissociation and fragmentation processes of furan in the gas phase. Thermal dissociation (pyrolysis) has been investigated by Lifshitz et al. [5] and Organ and Mackie [6] who performed single-pulse shock-tube experiments. More recently Fulle et al. [7] used the shock wave method over the extended temperature range, 500–3000 K, with laser-schlieren densitometry and TOF mass spectrometry detection techniques. Sorkhabi et al. [8] have studied photodissociation dynamics of furan at 193 nm using photofragment translational spectroscopy with mass analysis of the dissociation products. *Ab initio* theoretical investigations of unimolecular decomposition channels of furan have been carried out by Liu et al. [9] who performed high-level calculations within density functional theory and by Sendt et al. [10] who used combined quantum chemical techniques. The results of the above studies indicate three primary unimolecular dissociation processes which produce the following pairs of fragments: carbon monoxide CO and propyne $CH_3C{\equiv}CH$, acetylene C_2H_2 and ketene $CH_2{=}CO$ and formyl HCO and propargyl $CH{\equiv}C{-}CH_2$ radicals. The first two dissociation processes occur on the ground state of furan following internal conversion of energy on the potential energy surface. The third one most likely takes place on an excited energy surface. The most likely mechanism for the HCO and CO production channels has an initial step of C—O bond cleavage (Fig. 1) leading to the opening of the furan ring. Further, the above three unimolecular dissociation channels additionally involve migration of hydrogen atom along the furan ring. It is of note that a very similar unimolecular dissociation mechanism has been invoked in the spectroscopic studies of furan photoions [11]. This mechanism models formation of the corresponding $C_3H_4^+$, $C_2H_2O^+$ and $C_3H_3^+$ fragment ions from the parent $C_4H_4O^+$ cation in the three main processes of the 12–14 eV photon energy range.

Dissociative electron attachment is another process leading to cleavage of molecular bonds. It is considered to be a two-step process. Here, a temporary negative ion is initially formed through incident electron capture which then dissociates giving a stable negative ion and a neutral fragment. In furan, the following negative ions were observed by Sulzer et al. [12] in the electron energy range 5.5–13 eV: $(F{-}H)^-$ (negative furan ion with a loss of one hydrogen atom), C_4H^-, C_2HO^-, $C_3H_3^-$ and C_2H^-. These dissociation products involve cleavage of several bonds and possibly creation of new bonds. For example, the $C_3H_3^-$ anion and its corresponding HCO neutral fragment can be viewed as formed by the cleavage of O(1)–C(2) and C(4)–C(5) bonds in the temporary negative ion while

* Corresponding author. Tel.: +48 58 347 2284; fax: +48 58 347 2821.
E-mail address: mazub@mif.pg.gda.pl (M. Zubek).

1387-3806/$ – see front matter © 2008 Elsevier B.V. All rights reserved.
doi:10.1016/j.ijms.2008.04.010

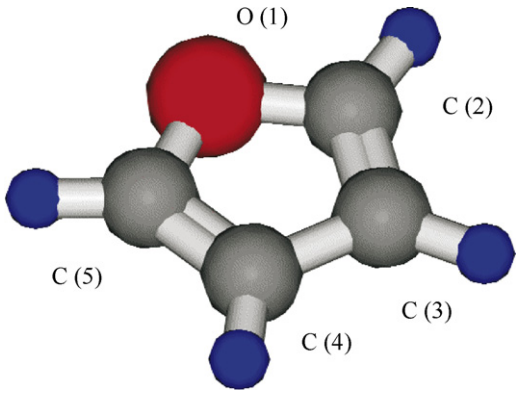

Fig. 1. Schematic diagram of furan, C_4H_4O molecule showing labeling of the atoms. The molecule belongs to the C_{2v} symmetry point group.

formation of C_2HO^- anion may involve cleavage of O(1)–C(2) and C(3)–C(4) bonds which is accompanied by hydrogen migration.

In the present work we have investigated dissociation and fragmentation processes in furan which lead to the formation of electronically excited neutral atomic and molecular fragments. The optical excitation technique, using electron impact, has been applied which allows identification of the dissociation and fragmentation species by detection of their fluorescence decay. The following excited fragments have been observed in the investigated electron energy range 15–95 eV: atomic hydrogen H(n) in the n = 4–10 states, the diatomic CH fragment in the $A^2\Delta$, $B^2\Sigma^-$ and $C^2\Sigma^-$ excited states and the C_2 fragment in the $d^3\Pi_g$ state. These atomic and molecular products differ from those previously reported and their observation gives new insight into the possible dissociation and fragmentation channels in furan.

2. Experimental

The electron spectrometer employed in the present measurements, which is shown in Fig. 2 is a further development of the apparatus described previously [13,14]. In the spectrometer the electron beam originating from a tungsten filament is formed by a trochoidal selector. A collimated beam with an energy spread of about 300 meV (FWHM) is accelerated to a required energy in the 15–95 eV range before entering the collision chamber. The electrons are guided by a magnetic field produced by a set of two coils placed outside of the vacuum chamber. The position of the coils is adjusted to ensure that the magnetic field is directed along the spectrometer axis. The electron beam is monitored by an electron collector. The spectrometer is equipped with a metastable detector for calibration purposes and observation of metastable fragments. Fluorescence from the collision region passes through a quartz light-guide and is focused on the entrance of the 0.25 m Ebert monochromator having 1181 lines/mm grating and is detected by a cooled photomultiplier.

The spectrometer has been operated in two modes. In the first mode, the fluorescence emission spectra were measured for fixed electron energy with an optical resolution ($\Delta\lambda/\lambda$) of 0.005. The wavelength scale was calibrated in mixtures of furan and nitrogen against the position of the (0,0) vibrational line (337.0 nm) of the second positive band of nitrogen to within ±0.2 nm. The obtained spectra were corrected for wavelength dependence of sensitivity of the optical detection channel. In the second mode of operation the wavelength of the detected emission was maintained fixed at a selected optical line and the excitation function of the emission was obtained in a given electron energy range. The intensity of the incident electron beam was typically 1–3 μA and was constant over the measured energy range to within ±8%. The collision path length variation with energy in the 20–100 eV range due to helical motion of electrons is estimated to be less than 10%. The electron energy

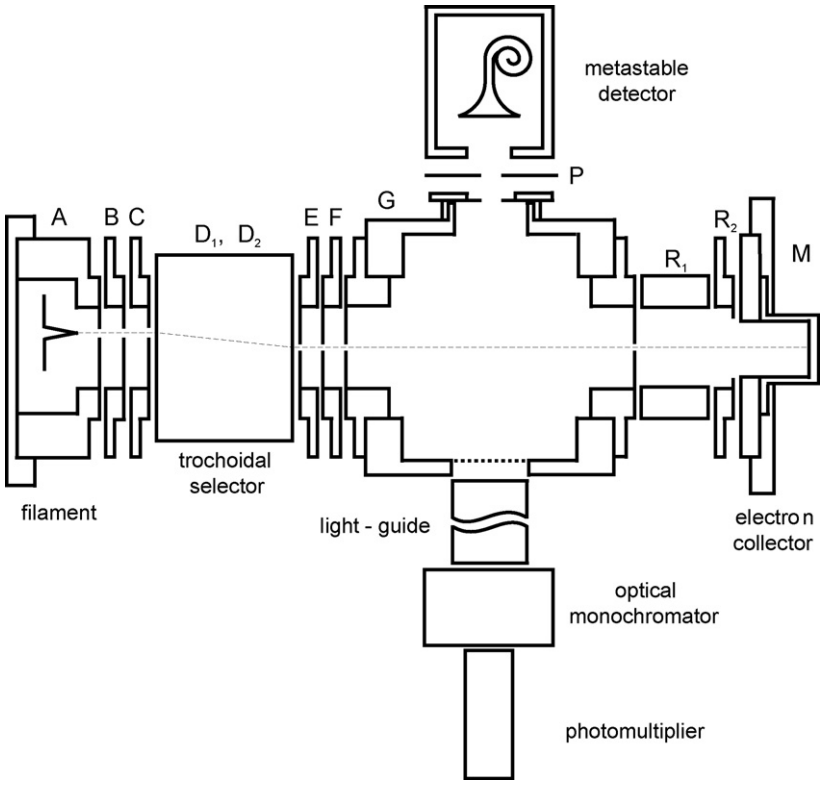

Fig. 2. Diagram of the electron impact optical excitation spectrometer. The electrodes of the spectrometer are shown to scale.

was calibrated against the position of the excitation threshold of the 337.0 nm line (11.03 eV) to within ±50 meV. All measurements were taken under conditions of linear dependence on target gas pressure and incident electron beam.

The absolute emission cross sections measured in this work in furan were determined using helium as a reference gas. The relative cross section of H_β line was normalized to an absolute value at 60 eV against the $3^3P \rightarrow 2^3S$ (388.9 nm) apparent emission cross section of 25×10^{-24} m^2 reported by van Raan et al. [15]. The cross section of the CH $A^2\Delta \rightarrow X^2\Pi_r$ emission, to account for rotational and vibrational excitation of the fragment was obtained by comparing the areas under the H_β and CH peaks in the fluorescence spectra. The area under the CH peak was determined by removing the H_γ contribution and integrating over the range 415–445 nm. No corrections for polarization of emitted radiation were applied. The polarization of the 388.9 nm line of helium at 60 eV is 15% [16] and the polarization of fluorescence following dissociation of molecules is typically less than 5%. The possible effects of polarization on the emission cross sections in the present measurements are smaller than the other sources of uncertainties. The total uncertainty in the absolute H_β emission cross section is estimated from the random uncertainty (25%) and that of helium emission cross-section (15%) to be 40%. The random uncertainty was taken as a maximum deviation from the average value in a series of measurements. The uncertainty in the CH emission cross section is somewhat higher due to contribution of the uncertainty in the peak areas ratio and we estimate here a total uncertainty of 50%.

Furan, with declared purity of 99% obtained form Aldrich, was degassed a few times in the vacuum container to remove the gaseous impurities before introducing into the collision region.

3. Results and discussion

The fluorescence spectra measured in furan in the 300–320 nm and 370–530 nm wavelength ranges, at the electron energy of 70 eV are shown in Fig. 3. The main spectrum of Fig. 3 contains the H_β up to H_ν lines of the Balmer series which reveal formation of hydrogen H(n) in the n = 4–10 states. It also shows emission at 430 nm and 390 nm of the CH fragments from the excited $A^2\Delta$ and $B^2\Sigma^-$ states, respectively, in their decay to the ground $X^2\Pi_r$ state. The inset of Fig. 3 displays additionally a weak emission of CH at 314 nm from the excited $C^2\Sigma^-$ state. The $A^2\Delta$ band is asymmetric and broadened at the base. This broadening results from overlapping

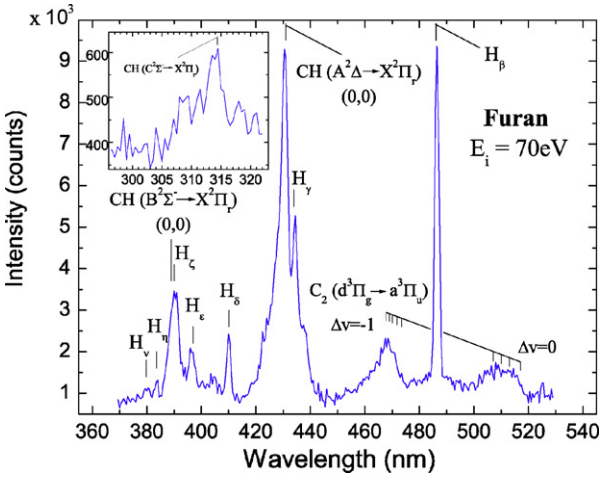

Fig. 3. Emission spectra obtained in furan at an incident electron energy E_i = 70 eV. The spectra were corrected for the wavelength dependence of the sensitivity of the optical detection channel.

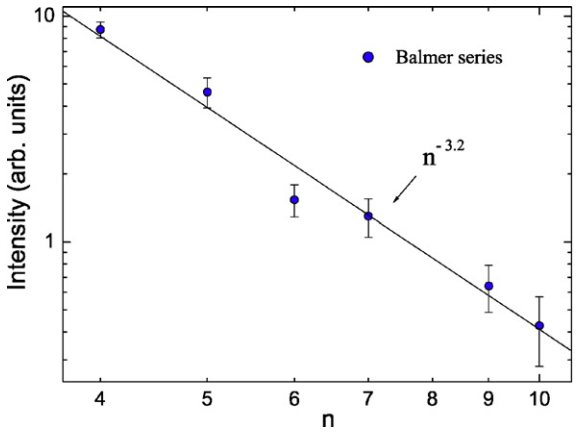

Fig. 4. The emission intensity of the Balmer series as a function of the n quantum number. The solid line shows the best fit to the experimental points of the $n^{-3.2}$ dependence.

rotational lines of the (0,0), (1,1) and (2,2) vibrational transitions and indicates high rotational excitation of the CH fragments. A similar CH emission spectrum obtained in ethylene with high optical resolution resolved rotational lines and its simulations gave a rotational temperature of about 4000 K for $v' = 0$ [17]. The $B^2\Sigma^-$ band of the CH emission (Fig. 3) is also asymmetric and wider than the hydrogen lines implying again rotational excitation of the fragment. Two broader emission peaks near 470 nm and 510 nm (Swan bands) show production of C_2 fragments in the excited $d^3\Pi_g$ state. These fragments are vibrationally excited as can be judged from the comparison with the positions of the single vibrational lines for $v' = 0$–5 and $\Delta v = -1, 0$. The C_2 fragments are also rotationally excited as shown by the tails on the rising slopes of the emission structures.

The intensity of the hydrogen Balmer lines from the spectrum of Fig. 3 are plotted against the n quantum number in Fig. 4. This dependence is approximated by a n^{-k} exponential function where k is a constant. From a least square fit to the experimental data $k = 3.2 \pm 0.3$ is obtained. This value of k gives n-dependence of the emission intensity that is comparable to the theoretical n^{-3} for the equal population of the excited hydrogen (n,l) substates [18].

We have determined appearance energies for formation of the H(n = 4) (H_β) and the CH($A^2\Delta$) (430 nm) fragments which are 20.7 ± 0.4 eV and 19.0 ± 0.3 eV, respectively. Details of the measurements in the energy region containing the appearance energies are shown in Fig. 5. The appearance energies which both are above the first ionization potential of furan (8.88 eV) can be compared with the estimated dissociation energies of the most probable processes. The hydrogen H(n = 4) fragment may directly result from abstraction of the atom from the furan ring (Fig. 1).

$$C_4H_4O \rightarrow C_4H_3O + H(n = 4). \quad (1)$$

The estimated dissociation energy of this process is 17.65 eV which is obtained from the C—H bond strength of 4.90 eV taken to be that of the benzene molecule [19] and the excitation energy of H(n = 4) states of 12.75 eV. In this process, the excess energy of 3.0 eV will appear as translational energy taken by the much lighter hydrogen atom, if there is no excitation of the remaining fragment in dissociation. It is interesting to note that translational energy of 3 eV was measured for H(n = 4) in dissociation of methane CH_4, which proceeds via excitation to a high-lying Rydberg state [20]. Production of H(n = 4) in furan may be considered, in analogy, as a two-body dissociation process of (1) with a mechanism of excitation of a Rydberg state converging to one of $7a_1^{-1}$, $6a_1^{-1}$ and $4b_2^{-1}$ ionic states in the 17–21 eV region. The other reactions producing hydrogen H(n = 4) would involve initial C—O bond cleavage requiring 3.39 eV

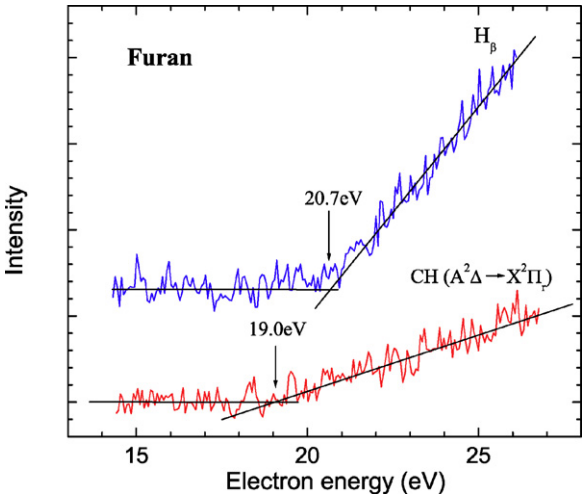

Fig. 5. Excitation functions of the H_β and CH $A^2\Delta \rightarrow X^2\Pi_r$ emissions showing appearance energy thresholds which are indicated by arrows.

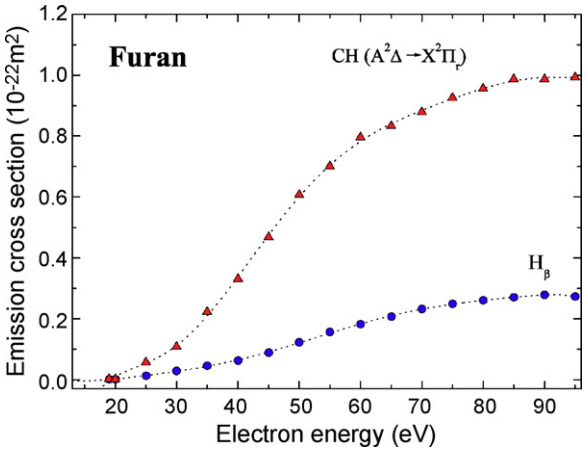

Fig. 6. Emission cross sections measured for the H_β line and CH $A^2\Delta \rightarrow X^2\Pi_r$ bands. The total uncertainties in these emission cross sections are 40% and 50%, respectively.

[7] and formation of an excited oxy-1,3-butadienylene intermediate diradical.

$$^{\bullet}CH = CH–CH = CH–O^{\bullet} \quad (2)$$

which next undergoes further decomposition. Here possible processes, analogous to those predicted for ground state tetrahydrofuran [21] for C(5)–O(1) bond cleavage, would involve H atom abstraction from the C(2) carbon accompanied by a simultaneous C(2)–O(1) π-bond formation or alternatively, but energetically less favorable, H atom abstraction from C(4) with a formation of C(4)–C(5) π-bond. Such processes may occur on the excited potential energy curves of diradical (2) producing excited H atoms in furan. The dissociation energies of these two reactions estimated using bond energies compiled in [22] are 17 eV and 18 eV, respectively. Further H(n = 4) producing reactions would need abstraction of hydrogen atom from C(3), C(4) or C(5) of the diradical (2) but these processes have dissociation energies above the presently measured appearance energy.

The CH($A^2\Delta$) fragments are produced from fragmentation of the diradical (2). The following processes have estimated dissociation energies below the measured appearance threshold of 19.0 eV.

$$C_4H_4O \rightarrow C_3H_3O + CH(A^2\Delta) \quad (3)$$

$$C_4H_4O \rightarrow C_3H_2O + CH(A^2\Delta) + H \quad (4)$$

$$C_4H_4O \rightarrow C_3HO + CH(A^2\Delta) + H_2 \quad (5)$$

$$C_4H_4O \rightarrow C_2H_2O + CH(A^2\Delta) + CH \quad (6)$$

$$C_4H_4O \rightarrow C_3H_3 + CH(A^2\Delta) + O. \quad (7)$$

For process (3) we obtain the lowest dissociation energy of 13.8 eV from excitation energy of the CH($A^2\Delta$) of 2.88 eV and the C=C bond strength of 7.54 eV [19]. Reaction (4) may proceed through different mechanisms, where abstraction of H atom involves additionally C—O or C—C π-bond formation. In reaction (5) a second C—H bond is broken to form an H_2 molecule. For process (6) we estimate dissociation energy of 17.1 eV. Processes (3) to (7) leave from about 2 eV to 5 eV into the translational and internal excitation of the fragments.

In this work we have also determined the absolute emission cross sections for the H_β line and the CH $A^2\Delta \rightarrow X^2\Pi_r$ bands in the 15–95 eV energy range which are shown in Fig. 6. Both cross sections increase smoothly above thresholds displaying behaviour typical for excitation of optically allowed states. No higher lying excitation thresholds were discerned on both curves; however they may include cascade contributions from higher lying excited states. The CH cross section at its maximum (Fig. 6) is comparable to that of 1.09×10^{-22} m^2 measured for cyclopropane, C_3H_6 at 100 eV [23] and the H_β cross section to 0.30×10^{-22} m^2 of *n*-butane, C_4H_{10} [24].

4. Conclusions

We have studied dissociation and fragmentation processes in furan which produce electronically excited neutral atomic and molecular fragments using electron impact optical excitation technique. The following excited fragments have been observed in the electron energy range 15–95 eV: atomic hydrogen H(n) in the n = 4–10 states, diatomic CH fragments in the $A^2\Delta$, $B^2\Sigma^-$ and $C^2\Sigma^-$ states and the C_2 fragments in the $d^3\Pi_g$ state. We have measured the appearance energies of the H(n = 4) and CH($A^2\Delta$) fragments and presented the first determinations of the absolute emission cross sections for H_β and CH $A^2\Delta \rightarrow X^2\Pi_r$ bands. Discussion of possible dissociation and fragmentation processes have indicated complexity of the reaction channels. Further experimental studies to establish correlations between products of the fragmentation are needed. Theoretical thermodynamic calculations should allow modeling of the fragmentation processes.

Acknowledgements

This work has been carried out within the European Science Foundation programme 'Electron Induced Processing at the Molecular level' (EIPAM) and COST Action CM0601. It is also partly supported by the Polish State Committee for Scientific Research.

References

[1] O. Meth-Cohn (Ed.), Comprehensive Heterocyclic Chemistry. The Structure, Reactions, Synthesis and Uses of Heterocyclic Compounds, vol. 1, Pergamon Press, Oxford, 1984.
[2] C.O. Kappe, S.S. Murphree, A. Padwa, Tetrahedron 53 (1997) 14179.
[3] S. Glenis, M. Benz, E. Legoff, J.L. Schindler, C.R. Kannerwurf, M.G. Kanatzidis, J. Am. Chem. Soc. 115 (1993) 12519.
[4] L. Sanche, Eur. Phys. J. D 35 (2005) 367.
[5] A. Lifshitz, M. Bidani, S. Bidani, J. Phys. Chem. 90 (1986) 5373.
[6] P.P. Organ, J.C.J. Mackie, J. Chem. Soc., Faraday Trans. 87 (1991) 815.
[7] D. Fulle, A. Dib, J.H. Kiefer, Q. Zhang, J. Yao, R.D. Kern, J. Phys. Chem. A 102 (1998) 7480.
[8] O. Sorkhabi, F. Qi, A.H. Rizvi, A.G. Suits, J. Chem. Phys. 111 (1999) 100.
[9] R. Liu, X. Zhou, L. Zhai, J. Comput. Chem. 19 (1998) 240.
[10] K. Sendt, G.B. Bacskay, J.C. Mackie, J. Phys. Chem. A 104 (2000) 1861.
[11] E.E. Rennie, C.A.F. Johnson, J.E. Parker, D.M.P. Holland, D.A. Shaw, M.A. MacDonald, M.A. Hayes, L.G. Shpinkova, Chem. Phys. 236 (1998) 365.

[12] P. Sulzer, S. Ptasinska, F. Zappa, B. Mielewska, A.R. Milosavljević, P. Scheier, T.D. Märk, I. Bald, S. Gohlke, M.A. Huels, E. Illenberger, J. Chem. Phys. 125 (2006) 044304.
[13] M. Zubek, J. Phys. B 27 (1994) 573.
[14] R. Olszewski, M. Zubek, Chem. Phys. Lett. 340 (2001) 249.
[15] A.F.J. van Raan, J.P. de Jongh, J. van Eck, H.G.M. Heideman, Physica 53 (1971) 45.
[16] I. Humphrey, J.F. Williams, E.L. Heck, J. Phys. B 20 (1987) 367.
[17] M. Tokeshi, K. Nakashima, T. Ogawa, Chem. Phys. 203 (1996) 257.
[18] H.A. Bethe, E.E. Salpeter, Quantum Mechanics of One- and Two-Electron Atoms, Plenum Press, New York, 1977.
[19] D.R. Lide (Ed.), CRC Handbook of Chemistry and Physics, CRC Press, Boca Raton, 2004.
[20] T. Ogawa, J. Kurowaki, M. Higo, Chem. Phys. 61 (1981) 181.
[21] A.A. Scala, E.W.-G. Diau, Z.H. Kim, A.H. Zewail, J. Chem. Phys. 108 (1998) 7933.
[22] S.J. Blanksby, G.B. Ellison, Acc. Chem. Res. 36 (2003) 255.
[23] G.R. Möhlmann, F.J. de Heer, Chem. Phys. 19 (1977) 233.
[24] J.M. Marendić, M.D. Tasić, J.M. Kurepa, Chem. Phys. 91 (1984) 273.